frontiers in Environmental Science

ORIGINAL RESEARCH
published: 21 March 2022
doi: 10.3389/fenvs.2022.823385

Geochemistry of the Dissolved Load of the Ramganga River, Ganga Basin, India: Anthropogenic Impacts and Chemical Weathering

Mohd Yawar Ali Khan[1], *Sugandha Panwar*[2,3]* *and Jie Wen*[4]

[1]Department of Hydrogeology, Faculty of Earth Sciences, King Abdulaziz University, Jeddah, Saudi Arabia, [2]Department of Earth Sciences, Indian Institute of Technology Roorkee, Roorkee, India, [3]State Key Laboratory of Marine Geology, Tongji University, Shanghai, China, [4]China Institute of Water Resources and Hydropower Research (IWHR), Beijing, China

The Ramganga basin is an important sub-catchment of the Ganga River to study the wide-scale effects of human-induced changes on geochemical processes. The basin inhabits pristine locations in the upstream and dense human establishments in the floodplain region. Furthermore, the entrapment of upstream sediments in the Kalagarh Dam aids in creating different geochemical regimes. To reveal the geochemical heterogeneity over the multi-spatial and temporal scale, controlling factors (natural and anthropogenic), and source end-members, dissolved load samples were collected during the pre-monsoon, monsoon, and post-monsoon season of the year 2014. Major cations and anions data were analyzed using principal component analysis and mass-balancing equations-based forward modeling to quantify the contribution from the atmosphere, rock weathering, and anthropogenic sources. The results show that chemical weathering predominates the dilution effect during the pre- and post-monsoon season. A high level of pollution prevails during the non-monsoon season and particularly in floodplain tributaries. Anthropogenic sources contribute up to 42% of the dissolved load composition, whereas silicate and carbonate weathering predominantly contributes 93 and 82% of the dissolved load. Further, the silicate weathering rate (4.9 t km^{-2} y^{-1}) is higher than the carbonate weathering rate and efficiently uptakes an average of 3.5 × 10^5 mol km^{-2} y^{-1} of CO_2. The findings revealed the extent of geochemical heterogeneity and controlling factors influencing the element flux, weathering rates, and chemical transportation over multi-spatial and temporal scales.

Keywords: Himalayan river, chemical weathering, Ramganga, forward model, provenance

OPEN ACCESS

Edited by:
Tarun Kumar Thakur, Indira Gandhi National Tribal University, India

Reviewed by:
Rudra Mohan Pradhan, Indian Institute of Technology Bombay, India
Saurabh Mishra, Hohai University, China

***Correspondence:**
Sugandha Panwar
sugandha.panwar@gmail.com

Specialty section:
This article was submitted to Freshwater Science, a section of the journal Frontiers in Environmental Science

Received: *27 November 2021*
Accepted: *02 February 2022*
Published: *21 March 2022*

Citation:
Khan MYA, Panwar S and Wen J (2022) Geochemistry of the Dissolved Load of the Ramganga River, Ganga Basin, India: Anthropogenic Impacts and Chemical Weathering. Front. Environ. Sci. 10:823385. doi: 10.3389/fenvs.2022.823385

INTRODUCTION

The chemical weathering processes in the Himalayan rivers have long been recognized as an important carbon sink influencing global climate. The Ganga River basin is an important terrestrial pool with an erosion rate of 2 mm $year^{-1}$ transporting 72.9 × 10^7 tons of sediments to the Bay of Bengal (Singh et al., 2006; Singh et al., 2008). The highlands and lowlands of the basin feature large geological, geomorphological, and anthropogenic divisions. Approximately, 90% of total physical erosion occurs in the rapidly exhuming high mountains which sources >65% of the sediment load from the Higher Himalayas (Singh et al., 2008). Whereas the Ganga alluvial plains (cover 80% of the

basin area) play an important role in the generation of large weathering fluxes. The study of Frings et al. (2015) highlights that 41% of the total silica mobilization occurs in the low-land areas, particularly in the alluvial plains. The coupling between erosion, weathering, and carbon cycle and contemporary silicate weathering rates and associated atmospheric CO_2 drawdown in the Ganga basin has been studied by the previous researchers (Gaillardet et al., 1999; Galy and France-Lanord, 1999; Galy et al., 2008; Singh et al., 2008; Galy and Eglinton, 2011; Bickle et al., 2018). However, few studies have attempted to quantify the chemical inputs from multiple sources (atmosphere, human, and rock weathering) (Rai et al., 2010; Tripathy and Singh, 2010; Panwar et al., 2016; Tsering et al., 2019).

In terms of land use–land cover, the Ganga river from its source to sink flows through diverse land cover extending from glaciated mountains to intensively cultivated floodplains. The mountainous terrain is sparsely populated, while ~43% of India's population resides in the alluvial plains which exert its influence on the river water quality. Rai et al. (2010) stated that anthropogenic activities can constitute upto 10% of the major ion fluxes even during the monsoon season when the dilution effect is high due to high runoff. The inflow of partial and untreated wastewater sourced from industrial, agricultural, and domestic sectors is a major concern for river contamination in North India (Kumar et al., 2021; Mishra et al., 2021). To prepare the conservation plan for restoring the water quality of the rivers in the Ganga basin, the knowledge of rates of the chemical reactions, sediment sources, and anthropogenic control in different geochemical regimes is important to be quantified.

The Ramganga River basin in NW India represents the ideal location to study the wide-scale effects of different climatic, geomorphological zones, and anthropogenic modifications partitioning the chemical weathering fluxes. The sub-catchment occupies 2.6% of the total Ganga Basin area and stretches from Kumaon Himalayas to the middle Ganga alluvial plains. Additionally, the presence of the Kalagarh Dam in the transition between the mountainous terrain and floodplain aids in creating different weathering regimes (Panwar et al., 2020). Based on anthropogenic perturbation Ramganga basin has been classified into three elevation clusters, from 1304 to 259 m, 207 to 154 m and 154 to 139 m as less polluted, moderately polluted, and heavily polluted, respectively (Khan et al., 2017). The distinct and variegated control of anthropogenic activities can impact the natural mechanism of erosion and flux transportation, thereby impacting the global sediment and carbon budget. To reveal the extent of geochemical heterogeneity and distinguish the processes influencing the element flux, weathering rates, and point and non-point source of dissolved load. This study aims to investigate the major ion composition of Ramganga and its tributaries to characterize the different end-members, and quantify the CO_2 consumption rate.

STUDY AREA

The Ramganga River is a significant tributary of the Ganga River that emerges from the Kumaon Himalayas in India (**Figure 1**). The catchment area is around 22,685 km^2, and the mean elevation is 1,530 m above the mean sea level (Khan et al., 2016; Khan et al., 2017; Khan and Wen, 2021). The river flows over a stretch of 642 km before the confluence with the Ganga River (Daityari and Khan, 2017; Khan, 2018). Physiographically, the river occupies two main segments: 1) mountainous terrain (outer and middle ranges of the Himalayas) characterized by steep hills and narrow and deep valleys (CWC, 2012) and 2) Ganga alluvial plain which covers approximately 85% of the total basin area. The land use–land cover (LULC) of the upper part of the basin includes the dominant presence of forest with fragmented habitation, well-known forest reserved area of Jim Corbett National Park, and the Kalagarh Dam at a junction of the Himalayan and floodplain unit, whereas the lower part of the basin includes densely populated, high crop growing and industrialized districts of Uttar Pradesh, viz., Rudrapur, Moradabad, and Bareilly (**Figure 2**, **Table 1**) (Khan et al., 2019).

Hydrological Setting

The Ramganga River is a spring and rain-fed river. The total annual rainfall in the basin is around 1,000 mm of which 80% occurs during the monsoon season (CWC, 2012). The river carries most of the annual water and sediment discharge during the monsoon season. Mean total suspended sediment concentration reported at Dabri during the monsoon is 2.43 $g\,L^{-1}$. The major tributaries of the river include Deota, Mandal, Kho, Phika, Dhela, Kosi, and Baigul (**Figure 1**).

Geology of the Ramganga Basin

The Ramganga basin in the Kumaon Himalayas features two major lithotectonic zones, namely Lesser Himalayas and Sub-Himalayas. The low- to high-grade metasediments of the Paleozoic to Mesozoic age with the unfossiliferous sequence cover Lesser Himalayas, whereas characterizing the molasse sediments of the Mid-Miocene to Pleistocene age, the major components of Sub-Himalayas are siltstone, sandstone clays, and boulders. Generally, the most significant lithologies in the Ramganga catchment are quartzites (Nagthat and Sandra formations), calcareous shales and siltstones (Blaini/Infrakrol formations), limestones (Krol and Deoband formations), low-grade metamorphics (phyllites, slates, and schists), and high-grade metamorphics (granite gneisses), etc. (Gupta and Joshi, 1990) (**Figure 2**). After covering the mountainous region of the Kumaon Himalayas, the river enters the Ganga alluvial plains formed by the accumulation of detritus from the Higher and Lesser Himalayas (Rai et al., 2010). The Quaternary lithostratigraphic sequence established in the descending order comprises 1) Ganga/Ramganga Recent Alluvium, 2) Ganga/Ramganga Terrace Alluvium, and 3) Varanasi Older Alluvium with two facies, i.e., sandy facies and silt clay facies; the first two comprise the Newer Alluvium (Khan & Rawat, 1990).

METHODOLOGY

The water samples from the Ramganga River and its tributaries were collected during three periods: pre-monsoon (March 2014),

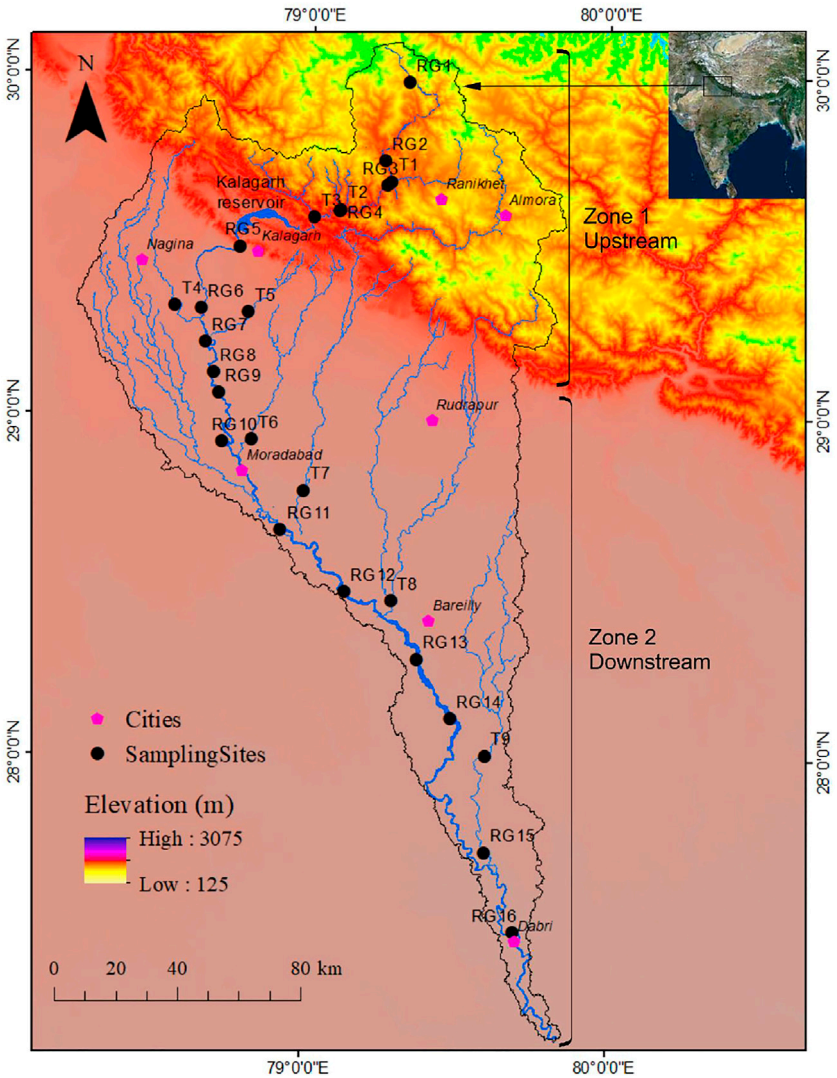

FIGURE 1 | Study area location with sampling sites (R1–R16 represent samples collected from the Ramganga River, T1- Gagas, T2- Deota, T3-Mandal, T4- Kho, T5- Phika, T6- Dhela, T7- Kosi, T8- Bhakra, and T9- Baigul).

monsoon (July 2014), and post-monsoon (November 2014). A five liter of water sample was collected in prerinsed polypropylene bottles from an approximate depth of 0.5 m. The tributaries were sampled ~1–3 km before their confluence with the Ramganga River. The sampling was carried out with utmost care following the standard protocols specified by Clesceri et al. (1998). The samples were filtered using pre-combusted cellulose nitrate membrane filters of 0.45 µm and were stored at <4°C before the analysis commenced.

The major ions were analyzed by ion chromatograph (Metrohm, 782 Basic IC), pH and HCO_3^- using an automatic titrator (Metrohm, 877 Titrino plus), and SiO_2 by UV spectrophotometer (Analytik Jena, Specord 250). The precision of these measurements was better than 5%. For accuracy purpose, the result of major ion composition was checked by specific charge balance as indicated by the normalized inorganic charge balance (NICB), sodium (Na^+) + potassium (K^+) + 2calcium (Ca^{2+}) + 2magnesium (Mg^{2+}) = 2sulfate (SO_4^{2-}) + chloride (Cl^-) + flouride (F^-) + bicarbonate (HCO_3^-) + nitrate (NO_3^-) (Jensen, 2003). All the results were within ±15% accuracy, except a sample RG16 (collected during monsoon time) which showed NICB of 18%.

To correctly process the multivariate dataset and bring out all the vital and important relationships between major cations and anions, principal component analysis (PCA) was applied using SPSS Statistics 2019 v26 software. PCA elucidates linear combinations between samples (represented by PC scores) and between variables (represented by PC loadings). The larger the loading value of a parameter, the greater the influence of that principal factor on the river composition. PCA was run on varimax rotation, and following the Kaiser principle, eigenvalues >1 were used to select significant components.

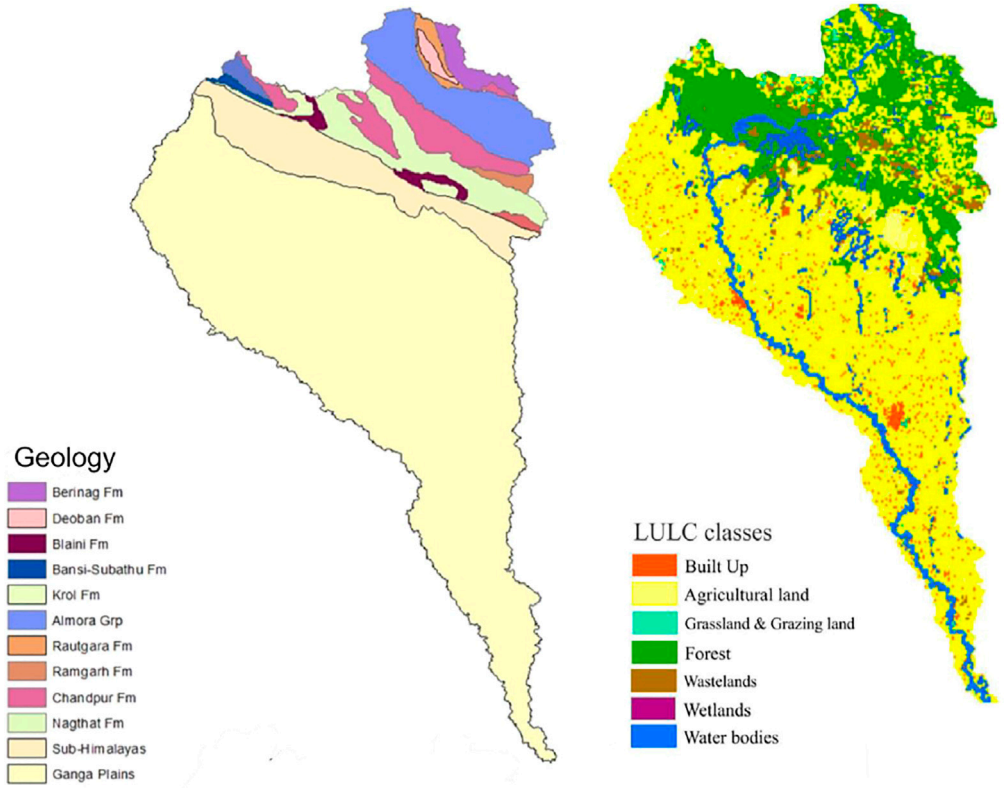

FIGURE 2 | Geological and land use land cover (LULC) map of the year 2014–2015 (Modified after Panwar et al. (2020)).

Atmospheric input	$Na_{rain} = (Na/Cl)_{rain}*Cl_{min}$ $Ca_{rain} = (Ca/Cl)_{rain}*Cl_{min}$	$K_{rain} = (K/Cl)_{rain}*Cl_{min}$ $Mg_{rain} = (Mg/Cl)_{rain}*Cl_{min}$
	Cl_{min}= lowest Cl in the river	
Anthropogenic input	For Zone 1, Anthropogenic% = NO_{3anth}/ΣAnions $NO_{3anth} = NO_{3river} - NO_{3rain}$	
	For Zone 2, $Cl_{anth} = Cl_{river} - Cl_{min}$ $Na_{anth} = (Na/Cl)_{anth}*Cl_{anth}$ $(Na/Cl)_{anth}$ of wastewater, $(K/Cl)_{anth}$ of wastewater	$K_{anth} = (K/Cl)_{anth}*Cl_{anth}$
Evaporite weathering	$SO_{4eva} = SO_{4river} - SO_{4rain}$	
Silicate weathering	For Zone 1, $Na_{sil} = Na_{river} - Na_{rain}$ $Mg_{sil} = (Mg/Na)_{silicate\ bedrock}*Na_{sil}$ $Ca_{sil} = (Ca/Na)_{silicate\ bedrock}*Na_{sil}$	$K_{sil} = K_{river} - K_{rain}$
	For Zone 2, $Na_{sil} = Na_{river} - Na_{anth} - Na_{rain}$ $Mg_{sil} = (Mg/Na)_{floodplain\ sediments}*Na_{sil}$ $Ca_{sil} = (Ca/Na)_{floodplain\ sediments}*Na_{sil}$	$K_{sil} = K_{river} - K_{anth} - K_{rain}$
Carbonate weathering	$Ca_{carb} = Ca_{river} - Ca_{sil} - Ca_{eva} - Ca_{rain}$ $Mg_{carb} = Mg_{river} - Mg_{sil} - Mg_{rain}$	

FIGURE 3 | Framework of the forward model depicting contribution from five reservoirs.

Furthermore, as postulated by Panwar et al. (2020), distinction in hydrological connectivity, physiography, and land use type promotes different sediment compositions in the upper (mountainous) and lower (floodplain) parts of the Ramganga basin. This feature is also well observed in the major element composition of the dissolved load (**Table 2**); hence, in this study, the river basin is divided into two parts, Zone 1 (upstream) and Zone 2 (downstream) with the man-made Kalagarh Dam located

TABLE 1 | Land use land cover (LULC) classes in the Ramganga basin.

LULC class	Area (km^2)
Built-up	497.508
Agriculture	15109.351
Grassland and grazing land	119.705
Forest	5896.264
Wasteland	341.481
Water bodies	721.284

in between. Zone 1 is defined as a mountainous silicate and carbonate rock-dominated zone, whereas Zone 2 is defined as an alluvial plain, urban-, industry-, and agriculture-intensive zone. A forward model based on mass budget equations of major cations (K^+, Na^+, Ca^{2+}, and Mg^{2+}) sourced from major reservoirs (atmosphere, lithology, and anthropogenic input) in Zone 1 and Zone 2 was employed. **Eq. 1** defines the mass budget equation for any element X:

$$X_{water} = X_{atm} + X_{eva} + X_{sil} + X_{carb} + X_{anth}, \quad (1)$$

where atm, eva, sil, carb, and anth refer to atmospheric input, evaporite dissolution, silicate weathering, carbonate weathering, and anthropogenic input, respectively.

But as the upper and lower Ramganga basin hosts different LULC patterns (**Figure 2**). In Zone 1, the forward modeling method mentioned by Li et al. (2019) was employed, whereas in Zone 2, the forward modeling approach followed by

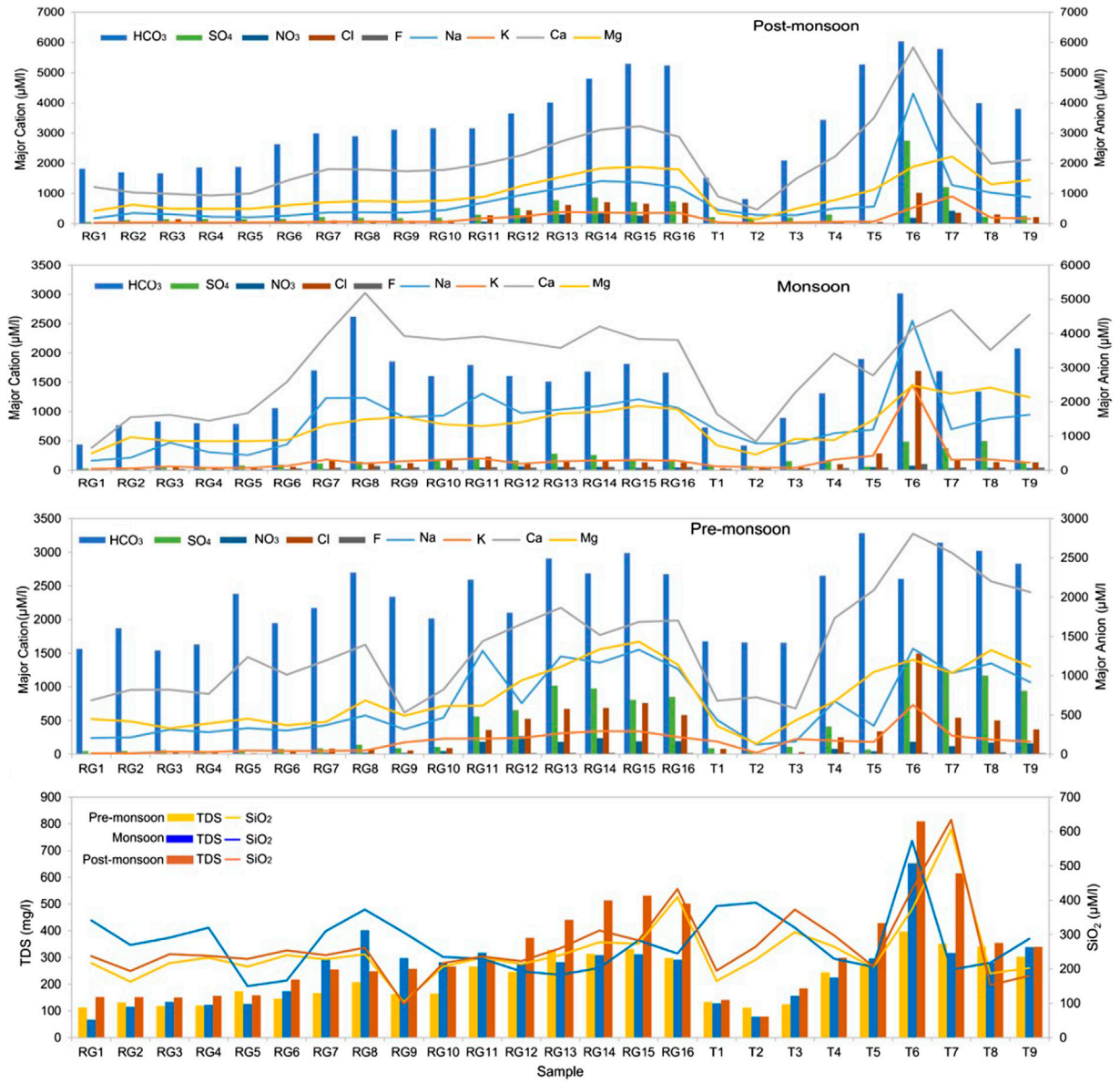

FIGURE 4 | Spatial and temporal variation in total dissolved solids (TDS), SiO_2, and major ions in the Ramganga River and its tributaries.

TABLE 2 | Statistics of major ion compositions of the Ramganga River and its tributaries (all data in μM except pH, total dissolved solids, TDS (in mg/l), and normalized inorganic charge balance, NICB (in %).

	pH	Na	K	Ca	Mg	F	Cl	NO_3	SO_4	HCO_3	NICB	SiO_2	TDS
Pre-monsoon													
Minimum	6.5	145.0	12.8	619.9	155.8	1.5	12.2	2.5	38.9	1323.6	-11.8	104	113
Maximum	8.0	1569.2	730.8	3275.4	1670.2	25.4	1281.9	229.6	1199.0	2816.2	12.9	606	397
Average	7.4	760.5	186.1	1614.3	863.3	8.9	264.0	74.9	381.1	2010.6	7.2	250	223
Standard deviation	0.4	500.7	156.6	752.4	449.6	7.9	304.1	78.0	398.1	471.1	6.3	97	91
Monsoon													
Minimum	7.1	162.1	23.7	382.3	267.8	23.7	35.6	1.6	39.2	723.7	-8.3	150	67
Maximum	8.3	2552.3	1458.3	3024.3	1447.4	182.5	2902.0	131.9	856.4	5174.5	18.2	573	652
Average	7.8	833.5	175.7	1804.1	794.1	72.1	303.6	48.8	284.9	2464.7	7.4	276	251
Standard deviation	0.3	498.8	274.9	747.7	337.5	34.0	554.4	38.8	221.4	1101.3	6.1	92	125
Post-monsoon													
Minimum	6.6	180.6	16.1	470.6	149.4	7.5	24.1	2.2	65.6	819.4	-10.9	98	79
Maximum	7.8	4306.7	903.5	5838.1	2223.7	42.7	1022.9	434.9	2750.0	6031.1	11.4	634	810
Average	7.3	783.0	179.2	2083.7	1006.1	15.4	260.8	86.2	441.8	3308.6	-2.6	268	317
Standard deviation	0.3	837.3	209.1	1163.2	584.3	9.2	277.2	131.4	563.6	1470.6	5.0	107	176
Annual													
Minimum	6.5	145.0	12.8	382.3	149.4	1.5	12.2	1.6	38.9	723.7	-11.8	98	67
Maximum	8.3	4306.7	1458.3	5838.1	2223.7	182.5	2902.0	434.9	2750.0	6031.1	18.2	634	810
Average	7.5	792.3	180.3	1834.0	887.8	32.1	276.1	70.0	369.3	2594.6	4.0	265	264
Standard deviation	0.4	624.8	216.0	917.3	470.3	35.2	393.7	91.2	417.8	1208.3	7.4	98	139

TABLE 3 | Varimax rotation PCA loading matrix.

Rotated component matrix		
	Component	
	1	2
Mg	.908	.213
Ca	.863	.253
SO_4	.855	.265
NO_3	.814	.134
HCO_3	.765	.299
Na	.752	.493
F	−.024	.812
Cl	.479	.759
K	.558	.703
SiO_2	.305	.597
Eigen value	6.188	1.178
Variance (%)	61.878	11.780
Cumulative variance (%)	61.878	73.657
Kaiser–Meyer–Olkin measure of sampling adequacy		.808

Chetelat et al. (2008) and Hua et al. (2020) was followed. The major ion composition of effluent samples carrying a mixed discharge of industrial and residential wastes mentioned in Sinha et al. (2006) and Gupta et al. (2018) was used as a wastewater sample.

Atmospheric dust can be a significant source of major ions in rainwater. In the absence of halite beds in the basin, the contribution of rainfall can be estimated by considering Cl^- as a reference element. Following Chetelat et al. (2008), Li et al. (2019), Hua et al. (2020), the lowest level of Cl^- was assumed to be sourced from the atmosphere.

Figure 3 shows the mass balance equations for each element with the assumptions. Furthermore, to estimate the silicate and carbonate weathering rates, water discharge data obtained from Central Water Commission, Middle Ganga Division, Lucknow, Uttar Pradesh, Government of India, were used.

RESULTS

River Water Chemistry

Table 2 lists the physiochemical parameters of the Ramganga River and its tributaries for pre-monsoon, monsoon, and post-monsoon seasons. The change of pH does not show any visible pattern in spatial and temporal context and varies from 6.5 to 8.3 (average 7.5), showing a slightly alkaline nature. The total anions and cations are 3,342 μeq/l to 3,694 μeq/l, in comparison to the global average of 1,200 μeq/l for river water (Meybeck, 1979). The total dissolved solids (TDS) during different seasons vary from 67 to 810 mg/L in comparison to adjacent Alaknanda basins (78–143 mg/L, Chakrapani et al., 2009) and the Ganga River at Rishikesh (89–226 mg/L, Chakrapani et al., 2009). The highest TDS of 810 mg/L was reported from the Dhela River (sample T6) during the post-monsoon season (**Figure 4**). A decrease in TDS in most of the samples during the monsoon season can be due to the dilution effect caused by high runoff, whereas an increase in the concentration of cations and anions in the non-monsoon season specifies that chemical weathering predominates the dilution effect in the non-rainy days. In all three seasons, Ca^{2+} is the major cation (average 1834 μM/L) with concentrations ranging

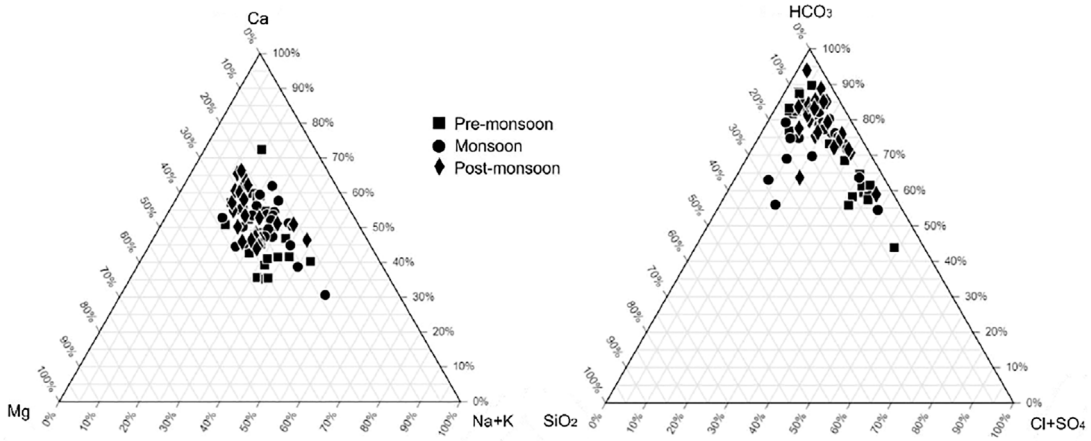

FIGURE 5 | Ternary diagrams of major cation and anion composition of the Ramganga River and its tributaries.

from 620 to 3,275 μM/L in pre-monsoon, 382–3,024 μM/L in monsoon, and 471–5,838 μM/L in post-monsoon seasons. The next common cations are Mg^{2+}, Na^{+}, and K^{+} having an average concentration of 888 μM/L, 792 μM/L, and 180 μM/L, respectively (**Figure 4**). The proportion of major ions is shown by ternary diagrams (**Figure 5**). The ternary diagram indicates the dominance of Ca^{2+} in all three seasons except samples T6 (Ca^{2+} 31%, Mg^{2+} 18%, and Na^{+}+K^{+} 51%) of monsoon time which shows dominance of Na^{+}+K^{+}. The dominance of Ca^{2+} and Mg^{2+} in all three seasons could be due to both silicate and carbonate weathering. The Na^{+}/Cl^{-} ratio >1 indicates that silicate weathering is quite strong in the basin. The geology of the basin indicates that Ca^{2+} and Mg^{2+} are sourced dominantly from the Lesser Himalayan formations, whereas Na^{+} and K^{+} are sourced dominantly from the felsic rocks.

HCO_3^{-} is the dominant anion with an average concentration of 2011 μM/L, 2,465 μM/L, and 3,309 μM/L in the pre-monsoon, monsoon, and post-monsoon seasons. The high concentration of HCO_3^{-} supports the presence of strong silicate weathering in the basin. The second dominant anion SO_4^{2-}accounts for 381 μM/L, 285 μM/L, and 442 μM/L in the pre-monsoon, monsoon, and post-monsoon seasons. As midstream and downstream of the Ramganga River is heavily under human control, the combined concentration of F^{-}, Cl^{-}, and NO_3^{-} accounts for 1.0%, 8.3%, and 2.1% of the total anions, respectively, and are related to the use of fertilizers in agriculture, sewage disposal, and industrial effluents. The ternary plot of HCO_3^{-}–SiO_2–Cl^{-}+SO_4^{2-} shows the clear dominance of SiO_2 and HCO_3^{-} in the anion budget. The presence of most of the sampling points along the mixing line of HCO_3^{-} and Cl^{-}+SO_4^{2-} indicates a contribution from Cl^{-} and SO_4^{2-}. Sample T6 from the pre-monsoon season shows that HCO_3^{-} accounts for 44%, SiO_2 for 7.3%, and Cl^{-}+SO_4^{2-} for 49% of the total anion share (**Figure 5**).

The concentration of dissolved silica varying from 98 μM/L to 634 μM/L (average 265 μM/L) is higher than the global river average of 145 μM/L (Meybeck, 2003), Amazon (60–160 μM/L,

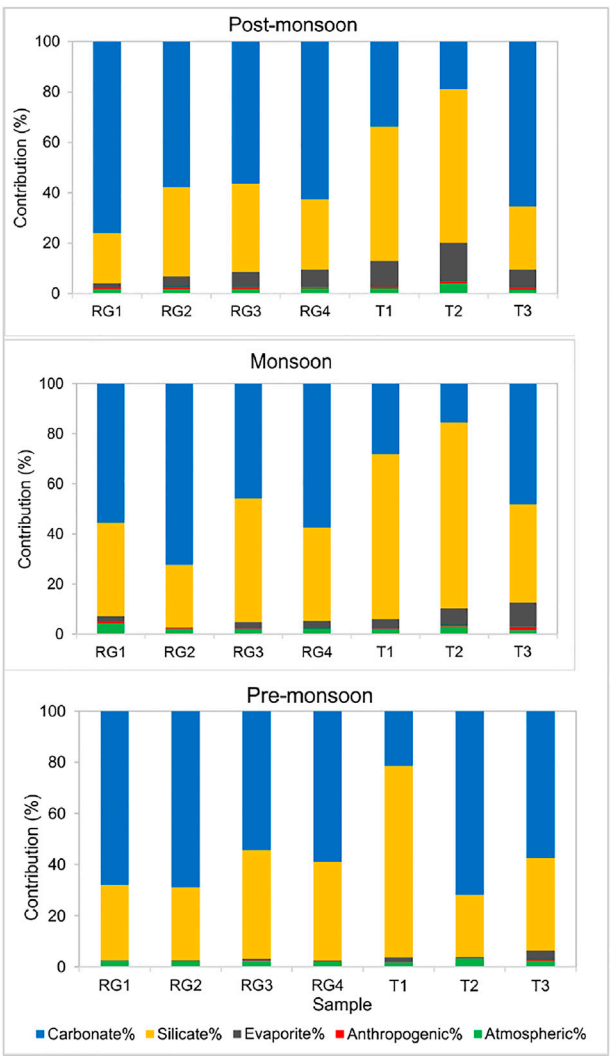

FIGURE 6 | Contribution of different sources to major cation load in pre-monsoon, monsoon, and post-monsoon season in upstream (Zone 1).

Gaillardet et al., 1997), Congo (140–210 μM/L, Dupre et al., 1996) River, and other tributaries of the Ganga River (59–135 μM/L in Alaknanda and 83–248 μM/L in Bhagirathi, Chakrapani et al., 2009), Yamuna (67–348 μM/L, Dalai et al., 2002). However, it is less than the Ganga mainstream at Farakka (average 318.6 μM/L, Bickle et al., 2018).

Principal Component Analysis

Table 3 shows the rotated component matrix generated to investigate and interpret intercorrelations between major ions and SiO_2. PC1 explains ~62% of the variance and shows positive loading on Mg^{2+}, SO_4^{2-}, Ca^{2+}, NO_3^-, HCO_3^-, and Na^+, moderately positive loading for Cl^- and K^+, and weak loading for SiO_2 (<0.5). PC2 explains ~12% of the variance in the dataset and shows positive loading for F^-, Cl^-, K^+, SiO_2, and Na^+.

DISCUSSION

Mixed Source of River Water

The intercorrelations between different components in PC1 and PC2 is hard to describe but suggest mixed sources of major ions, i.e., the contribution from multiple end-members, such as rock weathering, anthropogenic inputs, and tributaries contribution (Liu and Han, 2020). **Figures 6**, **7** show the relative contribution from different reservoirs estimated through the forward model.

Precipitation Input

Zone 1 is a pristine terrain with a sparse population and industrial activity. The contribution of rain inputs to dissolved loads in river are estimated by Cl-normalized ratios of rainwater. The lowest Cl^- concentration (12.88 μM/L) in sample T2 was assumed to be derived entirely from rainwater. The result shows that

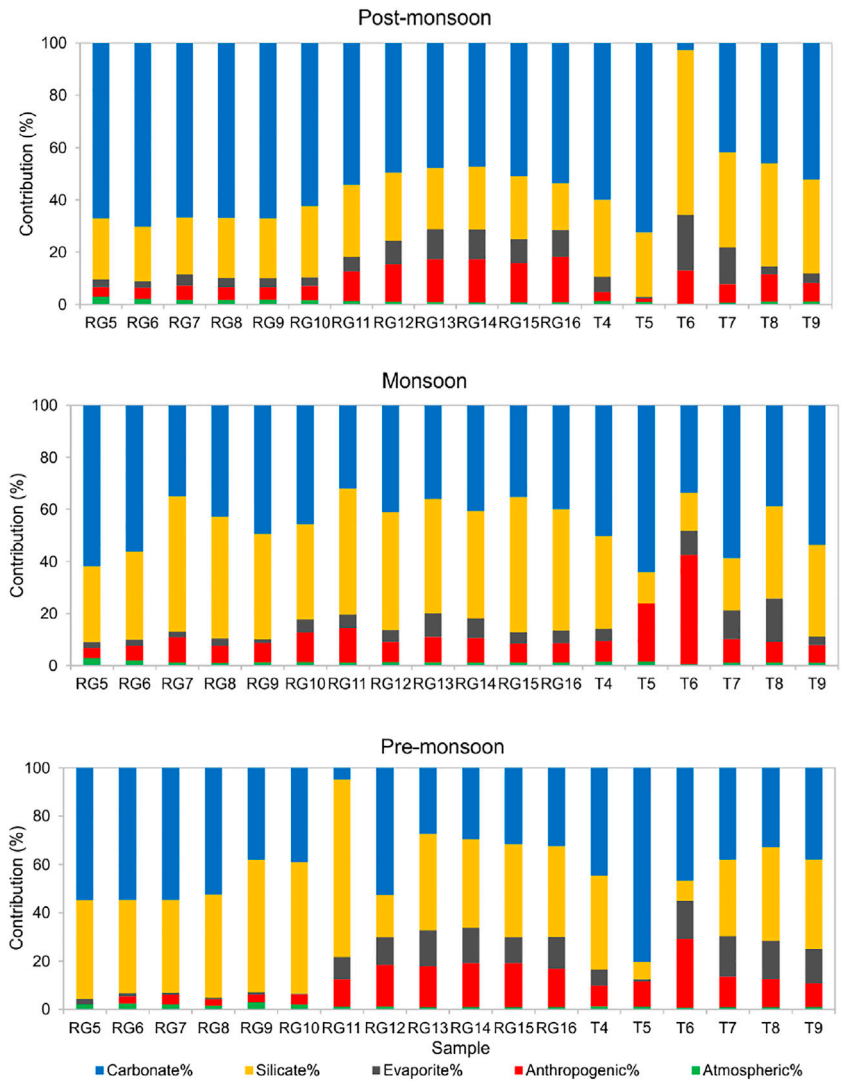

FIGURE 7 | Contribution of different sources to major cation load in pre-monsoon, monsoon, and post-monsoon seasons in floodplain region (Zone 2).

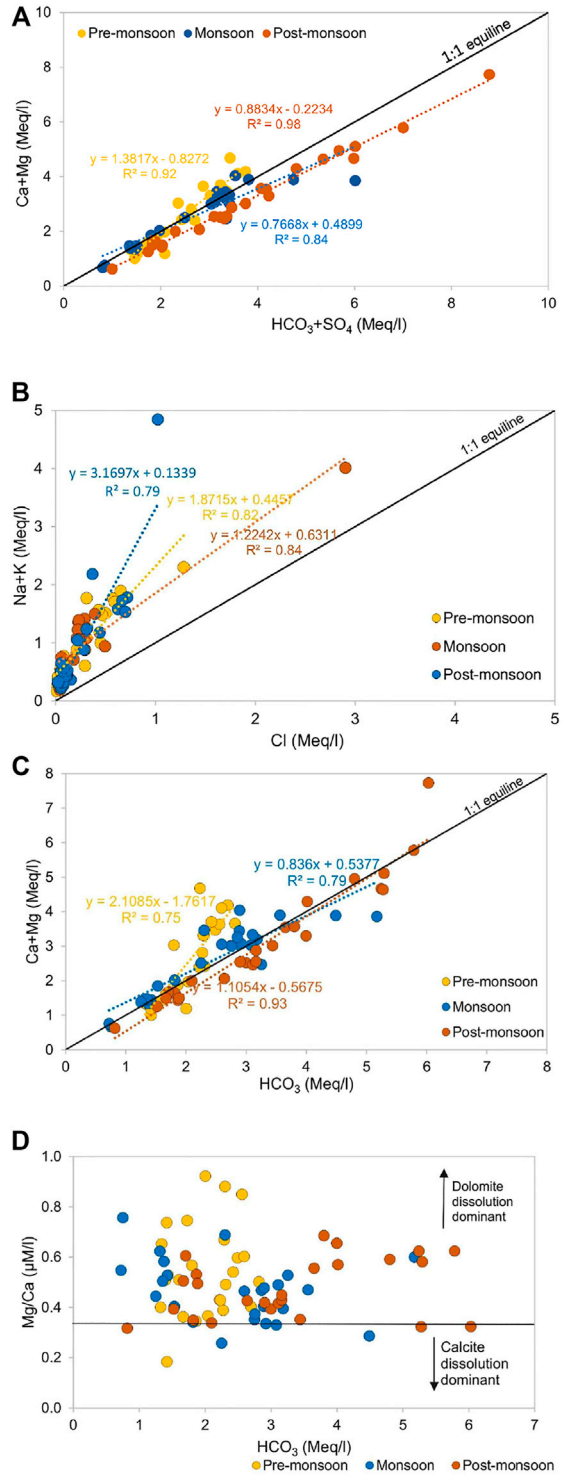

FIGURE 8 | Scatter plot of **(A)** HCO_3+SO_4 versus Ca + Mg, **(B)** Cl versus Na + K, **(C)** HCO_3 versus Ca + Mg, and **(D)** HCO_3 versus Mg/Ca revealing predominance of dolomite weathering.

atmospheric contribution in the mountainous part varies from 1.6 to 4.3% which is less than that in the adjacent Alaknanda basin (1.0–5.6%, Panwar et al., 2016) (**Figure 6**).

Zone 2 is polluted with agricultural, industrial, and urban effluents and limits the application of Cl^--normalized ratios of rainwater to quantify the atmospheric contribution. Therefore, the sampling point R5 was planned in the Kalagarh Forest Division. The sample R5 shows the minimum pollution level in the alluvial plains, and the lowest Cl^- concentration (12.19 µM/L) in pre-monsoon was assumed to be derived entirely from rainwater. Following the procedure mentioned in **Figure 3**, the estimated atmospheric contribution was found to vary between 0.4 and 2.9% (**Figure 7**).

Anthropogenic Contribution

The LULC map of the upper Ramganga basin displays the presence of terrace farming in the mountains (**Figure 2**). The cultivation in the region is mainly for subsistence purposes rather than commercial, thereby involving very low input of fertilizers (Pande et al., 2016). The low concentrations of Cl^- and NO_3^- in the upper Ramganga basin (Zone1) also indicate low anthropogenic control. However, the positive loading value for NO_3^- in factor 1 and F^- and Cl^- in factor 2 demands studying the impact of anthropogenic control in the entire basin (**Table 3**). Since Na^+, K^+, Ca^{2+}, and SO_4^{2-} are also a product of rock weathering, following the approach of Li et al. (2019), we considered NO_3^- as an indicator of human activities in the headwaters (Zone 1) and assumed that all NO_3^- comes from human activities. The results are comparable to Alaknanda and Teesta rivers which also do not show significant anthropogenic influence (Panwar et al., 2016; Tsering et al., 2019).

In Zone 2, the concentration of TDS, Na^+, K^+, SO_4^{2-}, Cl^-, and NO_3^- increases many fold times as the river enters the plains (**Figure 4**). The floodplains of Ramganga hub agricultural and industrial centers, both point sources (municipal and industrial wastewaters) and nonpoint sources (agricultural and irrigation runoff) can contribute majorly to dissolved loads. Therefore, in Zone 2, wastewater was used as an indicator of human activities. Na^+ and K^+ were used as a proxy for anthropogenic input as the addition of Ca^{2+} and Mg^{2+} from human activities is considered negligible in comparison with fluxes from rock weathering (Chetelat et al., 2008; Li et al., 2019). The presence of low Ca/Na (0.39) in the wastewater sample also indicates that Na constitutes a relatively large proportion of cations in the wastewater at Moradabad. The forward modelling results demonstrate that in the Ramganga mainstream (sample R5 to R16) anthropogenic input constitutes 9.5% ± 7.3%, 8.2% ± 2.6%, and 9.9% ± 5.6% in the pre-monsoon, monsoon and post-monsoon season (**Figure 7**). Similar to our results in the Ganga River, the low impact of anthropogenic input was observed during the monsoon season (Rai et al., 2010). However, the tributaries were found to carry more pollutants during the monsoon with a share of 16.0% ± 13.9%, in comparison to 13.5% ± 7.5% and 6.9% ± 4.2% during the pre-monsoon and post-monsoon season. The tributary Dhela (T6) was found to be most polluted carrying up to 42% of the anthropogenic input during the monsoon time. Our results specify that Ramganga is most polluted in the middle course

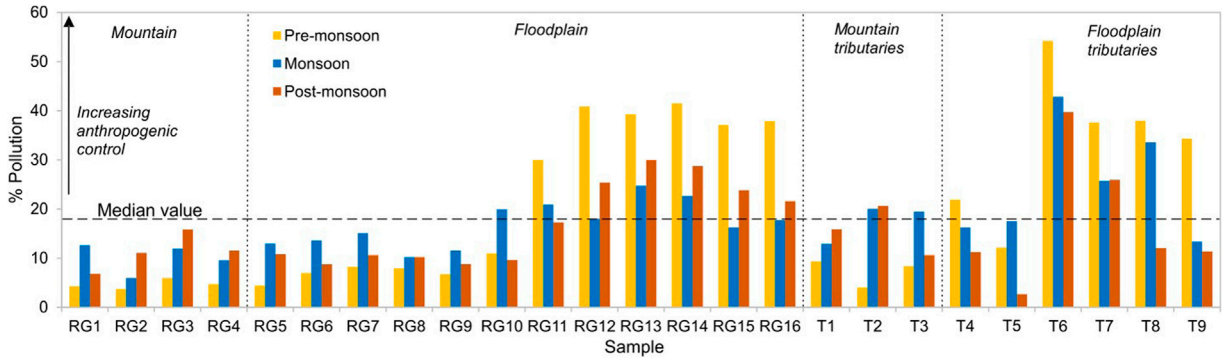

FIGURE 9 | Relative contribution of pollution to dissolved load composition. (Median value of floodplain samples was used to segregate the data).

as tributaries Phika (T5) and Dhela (T6) exert their influence on the river's geochemical composition.

Evaporites Weathering

Previous studies of Galy and France-Lanord (1999), Dalai et al. (2002), Chakrapani et al. (2009), Panwar et al. (2016) highlight the role of sulphide weathering as a source of SO_4^{2-} in the Himalayan basins. The strong positive correlation between $Ca^{2+}+Mg^{2+}$ and $HCO_3^-+SO_4^{2-}$ in all three seasons and the regression line close to equiline indicate the significant action of H_2SO_4 on carbonate weathering (**Figure 8A**). Furthermore, excess $HCO_3^-+SO_4^{2-}$ over $Ca^{2+}+Mg^{2+}$ indicates a non-carbonate source (Meyer et al., 2017; Tsering et al., 2019). The SO_4^{2-} in river water can be from multiple sources such as dissolution of sulfate evaporites, oxidation of sulphide minerals and organic S, and anthropogenic activities (Lang et al., 2006). A poor correlation between Cl^- and SO_4^{2-} (R^2 = 0.1) in Zone 1 and a weak correlation between Cl^- and SO_4^{2-} (R^2 = 0.3) indicate SO_4^{2-} is dominantly sourced from evaporite weathering and atmospheric deposition. Since no halite beds are present in the Ramganga basin, the concentration of K^+_{eva}, Na^+_{eva}, and Mg^{2+}_{eva} has been considered nil. In the Lesser Himalayas, the pyrite and gypsum deposits can be the probable source of SO_4^{2-} in the river water (Dalai et al., 2002; Chakrapani and Veizer 2006; Chakrapani et al., 2009). However, the estimation of the SO_4^{2-} fraction from pyrite is difficult to estimate in the Himalayan terrain as sulfuric acid is formed due to the oxidation of pyrite, which further participates in chemical weathering of silicate and carbonate rocks (Chakrapani and Veizer 2006). Therefore, after the correction of atmospheric and anthropogenic inputs, the remaining SO_4^{2-} considered to be derived from pyrite and gypsum weathering was found to vary from 0.1 to 15.3% in Zone 1 and 0.1–21.1% in Zone 2.

Silicate Weathering

Figure 8B shows all samples lie above the equiline and thus indicates the dominance of silicate weathering in the basin. To quantify the silicate contribution to major cations, Cl^- concentration corrected for anthropogenic activities and atmospheric input is used as an index. In the absence of halite beds in the study area, silicate weathering is considered the biggest contributor of Na^+. Similarly, K^+ is also considered to be derived from silicate as carbonates, and evaporites have a minimum amount of K^+.

As silicate weathering can release an appreciable amount of Ca^{2+} and Mg^{2+}. In the absence of Ca/Na and Mg/Na data from ideal monolithologic streams, the molar ratio of Ca/Na = 0.7 and Mg/Na = 0.3 mentioned in Krishnaswami & Singh (1998) and Dalai et al. (2002) was used for the mountainous terrain

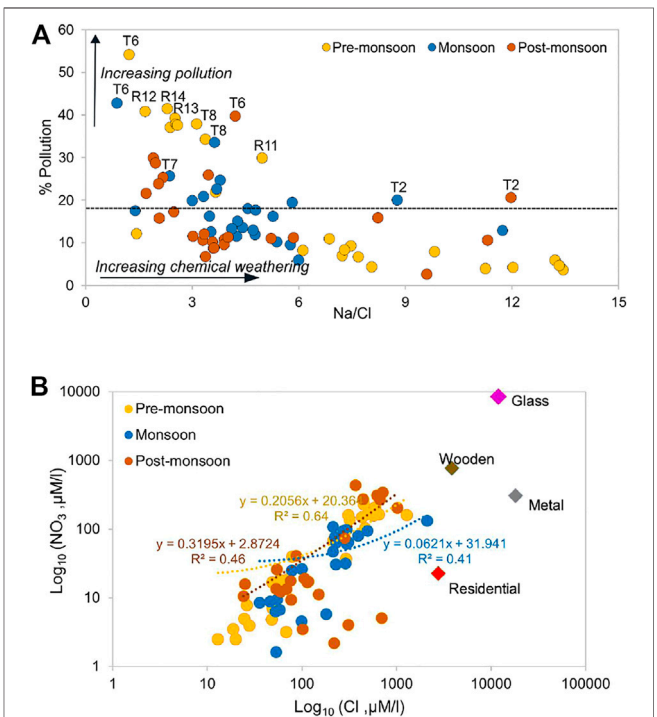

FIGURE 10 | (A) Pollution percentage versus Na/Cl showing high pollution in the downstream tributaries (dashed line indicate median value of floodplain samples), and **(B)** Cl versus NO_3, data of urban sources and industries were adapted from the Joint Inspection Report, National Green Tribunal Report, 2019.

(Zone 1), whereas for the floodplain sediment, the average ratio of Ca/Na = 0.91 and Mg/Na = 0.56 at different locations mentioned in Tripathi et al. (2007) was used. The results show that silicate weathering contributed ~41% of the dissolved load in Zone 1 and ~35% in Zone 2. The decrease in the silicate weathering rate as the river traverses downstream is contradictory to the Ganga floodplain region where ~41% of the initial silica mobilization occurs (Frings et al., 2015; Bickle et al., 2018).

Carbonate Weathering

The carbonate is abundant as a diagenetic cement in the floodplain sediments and seems to have a major influence on the river composition (Bickle et al., 2018). The high concentrations of Ca^{2+} and Mg^{2+} and strong positive correlation between Ca^{2+}+Mg^{2+} and HCO_3^- indicate carbonate weathering to be a dominant source of these ions (**Figure 8C**). The forward modeling shows that combined dolomite and limestone weathering contributes 52% of the dissolved load in Zone 1 and 47% in Zone 2 with maximum dissolution during the non-monsoon season. The Mg^{2+}/Ca^{2+} ratio can help to discriminate the relative proportion of calcite and dolomite dissolution. A ratio of 0.33 indicates the equal molar dissolution of calcite and dolomite (Szramek et al., 2007). In all three seasons, the Mg^{2+}/Ca^{2+} ratio of 0.5 and plot between Mg/Ca and HCO_3 (**Figure 8D**) suggest that dolomite dissolution is favored over calcite dissolution and contributes majorly to total dissolved loads of HCO_3^- and Ca^{2+}.

Anthropogenic Source of Pollution

Since anthropogenic activities significantly contribute to the dissolved load composition of the Ramganga River, we elucidate the spatial context of pollution throughout the river course. The percentage of pollution was estimated following Pacheco and Van der Weijden (1996):

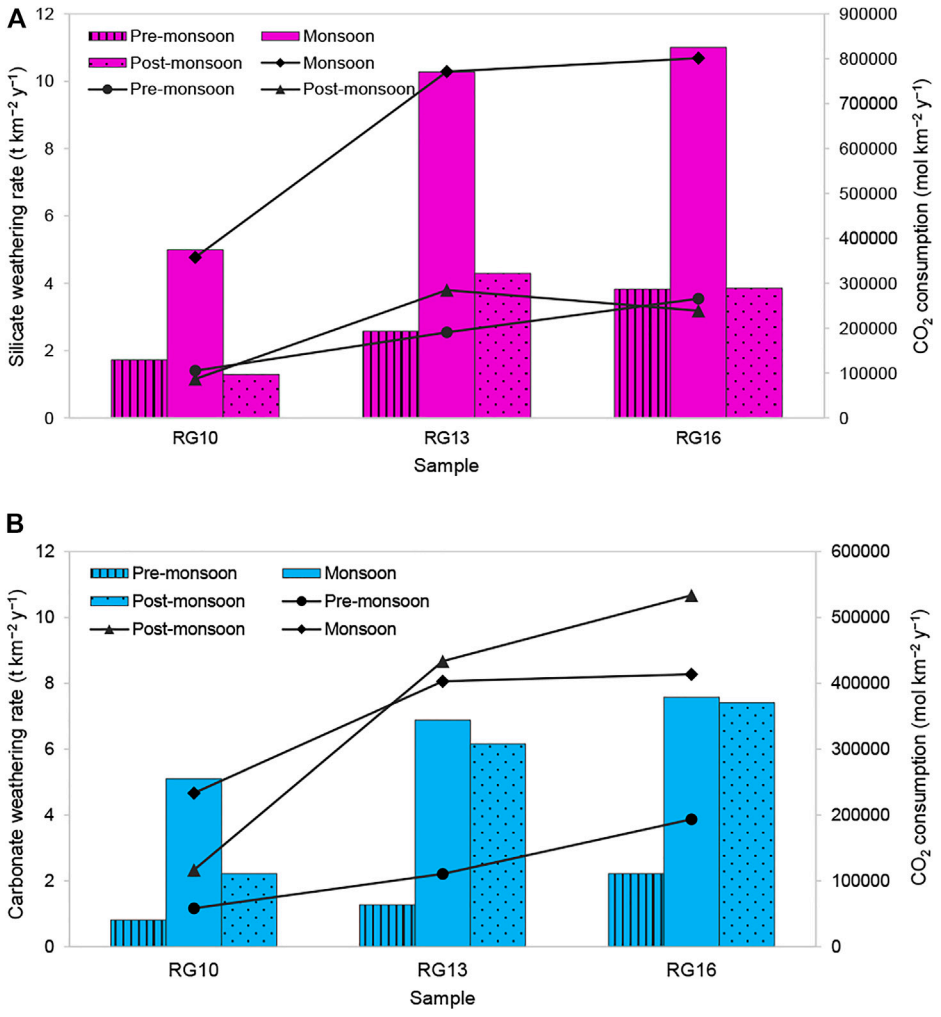

FIGURE 11 | (A) Silicate weathering rate (SWR) and resultant CO_2 consumption, **(B)** carbonate weathering rate, (CWR) and resultant CO_2 consumption (column indicates weathering rate and line + scatter display CO_2 consumption rate).

$$\%\ pollution = \frac{[Cl^-] + [SO_4^{2-}] + [NO_3^-]}{[Cl^-] + [SO_4^{2-}] + [NO_3^-] + [HCO_3^-]} \times 100,$$

where the anion concentrations are in meq/l.

The median value of floodplain samples was used to segregate the dataset. The samples having ratios ≥18% were considered dominated by pollution from anthropogenic activities, while those with ≤18% depicted the limit of rock weathering **(Figure 9)**. The results show a significantly high level of pollution during the non-monsoon season and high contamination loads after sample R10 as the river passes through the industrial town of Moradabad which braces glass, metal, and wooden industries. Samples R12 and R14 show a pollution index of >40% in the pre-monsoon season. The high value in the samples T6-T8 during the monsoon shows the impact of tributaries on the Ramganga mainstream throughout the year. Tributaries particularly T6 (Phika) highlight an adverse level of pollution with an average % pollution index of 46% throughout the year. On average, the percentage of pollution in upstream tributaries (T1 to T3) stands at 13.5%, whereas in floodplains tributaries (T4 to T9) it is ~25%. The plot between % pollution and Na^+/Cl^- indicates that in samples R12 to R14, and T6 contribution of major anions, especially Cl^- is dominantly sourced from anthropogenic activities (**Figure 10A**). Furthermore, a low NO_3/Cl ratio (0.26) and Cl^- versus NO_3^- plot indicate the impact of untreated residential sewage effluent on the river composition (**Figure 10B**) even though agriculture is a dominant land cover in the lower Ramganga basin. The study of Panwar et al. (2020) mentions the presence of high coercivity antiferromagnetic minerals in the tributaries Pheka and Dhela and related it to industrial and agricultural pollutants in the rivers. Our results ratify that pollution in tributaries majorly influences the chemical composition of the Ramganga River in the floodplain region.

Weathering Rates and CO_2 Consumption Flux

To estimate the efficiency of chemical weathering processes, the silicate weathering rate (SWR) and carbonate weathering rate (CWR) were calculated. The SWR and CWR were calculated in Zone 2 as daily water discharge data were available only for three locations–Moradabad (RG10), Bareilly (RG13), and Dabri (RG16). SWR and CWR were estimated for pre-monsoon, monsoon, and post-monsoon as follows:

$$\mathrm{SWR} = \left(Ca_{sil}^{2+} + Mg_{sil}^{2+} + K_{sil}^{+} + Na_{sil}^{+} + SiO_2\right) \times \frac{\text{discharge}}{\text{drainage area}}; \quad (2)$$

$$\mathrm{CWR} = \left(Ca_{carb}^{2+} + Mg_{carb}^{2+}\right) \times \frac{\text{discharge}}{\text{drainage area}}. \quad (3)$$

(Figure 11) shows the SWR and CWR in the basin. The average SWR in the Ramganga alluvial plains (4.9 t km^{-2} y^{-1}) was found to be lower than that in the Ganga River (10.2–15.2 t km^{-2} y^{-1}) but higher than that in the Indus (3.8 t km^{-2} y^{-1}, Gaillardet et al., 1999). The CWR varies from 0.8 to 7.6 t km^{-2} y^{-1} in the Ramganga floodplains. The highest CWR was observed at Dabri (5.7 t km^{-2} y^{-1}). The increase in CWR from R10 to R16 can be attributed to the contribution from tributaries (T7 to T9) that flow from the carbonate outcrops in the Himalayas contributing a significant amount of Ca and Mg.

The CO_2 consumption through silicate and carbonate weathering (CSW) was calculated using the following equations:

$$[CO_2]_{SW} = \left(K_{sil}^{+} + Na_{sil}^{+} + 2Ca_{sil}^{2+} + 2Mg_{sil}^{2+}\right) \times \frac{\text{discharge}}{\text{area}}; \quad (4)$$

$$[CO_2]_{CW} = \left(Ca_{carb}^{2+} + 2Mg_{carb}^{2+}\right) \times \frac{\text{discharge}}{\text{area}}. \quad (5)$$

The CO_2 consumption rate is higher in silicate weathering than that in the carbonate weathering. CO_2 consumption fluxes deduced from silicate weathering range from 8.7×10^4 to 8.0×10^5 mol km^{-2} $year^{-1}$(average annual 3.5×10^5 mol km^{-2} $year^{-1}$) is 3.5 times the global average of about 1×10^5 mol km^{-2} $year^{-1}$ (Gaillardet et al., 1999). It is lower than those of the adjacent mountainous Bhagirathi–Alaknanda basins (4×10^5 mol km^{-2} $year^{-1}$), Yamuna (5.5×10^5 mol km^{-2} y^{-1}), and Brahmaputra (5.2×105 mol km^{-2} y^{-1}); however, it is higher than the Indus basin (0.6×10^5 mol km^{-2} y^{-1}). The CO_2 consumption through carbonate weathering ranges from 5.8×10^4 to 5.3×10^5 mol km^{-2} y^{-1} with the highest uptake during the post-monsoon season.

The occurrence of the highest SWR and CO_2 consumption in the monsoon season relates to the coupling between physical erosion and chemical weathering processes. The increase in SWR and CWR as the river flows downstream (R10–R16) relates to enhanced water discharge. The dissolved load of the river increases due to contributions from tributaries. The dissolved load at Dabri (RG16) is ~10 times that at Moradabad (RG10), as major tributaries such as Kosi (T7), Bhakra (T8), and Baigul (T9) join the river. Additionally, high runoff due to high-intensity rainfall, appropriate increment in temperature (average annual temperature is 24.1°C, 24.5°C, and 25°C at Moradabad, Bareilly, and Dabri in Kannauj, respectively), and morphology of the study area (Ganga plains having 9.5 cm km^{-1} of the average slope; Shrivastava, 1999), are other major factors controlling the silicate weathering and resultant CO_2 sequestration.

CONCLUSION

The Ramganga River flows through different geochemical regimes influenced by natural and anthropogenic activities. The total dissolved solids (TDS) show large spatial and temporal variations and vary from 67 to 810 mg/L. The major ions are present in the following order: $Ca^{2+} > Mg^{2+} > Na^+ > K^+$ and $HCO_3^- > SO_4^{2-} > Cl^- > NO_3^- > F^-$. The percentage of pollution is high in the samples downstream of Moradabad city (R10) and were found to be influenced by floodplains tributaries. Among all the samples, Dhela River (sample T6) was found to be the most polluted. The forward model quantifies the contribution from different sources in the following order: carbonate > silicate > evaporite > atmosphere > anthropogenic in Zone 1 and carbonate > silicate > evaporite > anthropogenic > atmosphere in Zone 2. In the upstreams, silicate weathering, contributed ~41% of the dissolved load, whereas in the floodplains its share is ~34% of the major cation load. Though carbonate weathering is quite strong in the basin, silicate weathering processes efficiently uptake more atmospheric CO_2. The silicate weathering rate (SWR) in the Ramganga floodplains

(1.3 – 11.0 t km^{-}2 year^{-1}) was found to be lower than the Ganga River. To restore the ecological assimilative capacity of the Ramganga River, we suggest specific policies should be formulated for different tributaries, especially for Phika, Dhela, and Kosi River. Furthermore, we advocate a large scale interdisciplinary study (involving the collection of soil, fertilizer and industrial effluent samples) to understand the effect of pollution on the dissolved load of the river.

DATA AVAILABILITY STATEMENT

The original contributions presented in the study are included in the article/supplementary material; further inquiries can be directed to the corresponding author.

AUTHOR CONTRIBUTIONS

MYAK and SP collected the data; SP and MYAK wrote the manuscript; SP revised and edited the manuscript and; JW helped in statistical analysis.

ACKNOWLEDGMENTS

This project was funded by the Deanship of Scientific Research (DSR) at King Abdulaziz University Jeddah, under Grant no. G: 207-145-1442. The authors, therefore, acknowledge with thanks to DSR for technical and financial support.

REFERENCES

Bickle, M. J., Chapman, H. J., Tipper, E., Galy, A., De La Rocha, C. L., and Ahmad, T. (2018). Chemical Weathering Outputs from the Flood plain of the Ganga. *Geochimica et Cosmochimica Acta* 225, 146–175. doi:10.1016/j.gca.2018.01.003

Chakrapani, G. J., Saini, R. K., and Yadav, S. K. (2009). Chemical Weathering Rates in the Alaknanda-Bhagirathi River Basins in Himalayas, India. *J. Asian Earth Sci.* 34 (3), 347–362. doi:10.1016/j.jseaes.2008.06.002

Chakrapani, G. J., and Veizer, J. (2006). Source of Dissolved Sulphate in the Alakananda–Bhagirathi Rivers in the Himalayas. *Curr. Sci.* 90 (4), 500–503. doi:10.1016/j.gca.2006.06.100

Chetelat, B., Liu, C.-Q., Zhao, Z. Q., Wang, Q. L., Li, S. L., Li, J., et al. (2008). Geochemistry of the Dissolved Load of the Changjiang Basin Rivers: Anthropogenic Impacts and Chemical Weathering. *Geochimica et Cosmochimica Acta* 72 (17), 4254–4277. doi:10.1016/j.gca.2008.06.013

Clesceri, L. S., Greenberg, A. E., and Eaton, A. D. (1998). *Standard Methods for the Examination of Water and Wastewater*. 20th ed. Washington, DC: American Public Health Association.

CWC (2012). *Environmental Evaluation Study of Ramganga Major Irrigation Project*, Vol. 1. R.K. Puram, New Delhi: Central Water Commission.

Daityari, S., and Khan, M. Y. A. (2017). Temporal and Spatial Variations in the Engineering Properties of the Sediments in Ramganga River, Ganga Basin, India. *Arab J. Geosci.* 10 (6), 134. doi:10.1007/s12517-017-2915-2

Dalai, T. K., Krishnaswami, S., and Sarin, M. M. (2002). Major Ion Chemistry in the Headwaters of the Yamuna River System:. *Geochimica et Cosmochimica Acta* 66 (19), 3397–3416. doi:10.1016/s0016-7037(02)00937-7

Das, P., Sarma, K. P., Jha, P. K., Ranjan, R., Herbert, R., and Kumar, M. (2016). Understanding the Cyclicity of Chemical Weathering and Associated CO2 Consumption in the Brahmaputra River Basin (India): The Role of Major Rivers in Climate Change Mitigation Perspective. *Aquat. Geochem.* 22 (3), 225–251. doi:10.1007/s10498-016-9290-6

Dupré, B., Gaillardet, J., Rousseau, D., and Allègre, C. J. (1996). Major and Trace Elements of River-Borne Material: The Congo Basin. *Geochimica et Cosmochimica Acta* 60 (8), 1301–1321. doi:10.1016/0016-7037(96)00043-9

Frings, P. J., Clymans, W., Fontorbe, G., Gray, W., Chakrapani, G. J., Conley, D. J., et al. (2015). Silicate Weathering in the Ganges Alluvial plain. *Earth Planet. Sci. Lett.* 427, 136–148. doi:10.1016/j.epsl.2015.06.049

Gaillardet, J., Dupré, B., and Allègre, C. J. (1999). Geochemistry of Large River Suspended Sediments: Silicate Weathering or Recycling Tracer? *Geochimica et Cosmochimica Acta* 63 (23-24), 4037–4051. doi:10.1016/s0016-7037(99)00307-5

Gaillardet, J., Dupre, B., Allegre, C. J., and Négrel, P. (1997). Chemical and Physical Denudation in the Amazon River Basin. *Chem. Geology.* 142 (3-4), 141–173. doi:10.1016/s0009-2541(97)00074-0

Galy, A., and France-Lanord, C. (1999). Weathering Processes in the Ganges–Brahmaputra basin and the Riverine Alkalinity Budget. *Chem. Geology.* 159 (1-4), 31–60. doi:10.1016/s0009-2541(99)00033-9

Galy, V., and Eglinton, T. (2011). Protracted Storage of Biospheric Carbon in the Ganges-Brahmaputra basin. *Nat. Geosci* 4 (12), 843–847. doi:10.1038/ngeo1293

Galy, V., France-Lanord, C., and Lartiges, B. (2008). Loading and Fate of Particulate Organic Carbon from the Himalaya to the Ganga-Brahmaputra delta. *Geochimica et Cosmochimica Acta* 72 (7), 1767–1787. doi:10.1016/j.gca.2008.01.027

Gupta, A., Tiwari, A., Tiwari, A., Pathak, A. P., and Tripathi, A. (2018). Experimental and Computational Approaches for Assessment, Bio-Degradation and Detoxification of Paper Industry Effluents. *Jebas* 6 (2), 425–436. doi:10.18006/2018.6(2).425.436

Gupta, R. P., and Joshi, B. C. (1990). Landslide hazard Zoning Using the GIS Approach-A Case Study from the Ramganga Catchment, Himalayas. *Eng. Geology.* 28, 119–131. doi:10.1016/0013-7952(90)90037-2

Hua, K., Xiao, J., Li, S., and Li, Z. (2020). Analysis of Hydrochemical Characteristics and Their Controlling Factors in the Fen River of China. *Sustain. Cities Soc.* 52, 101827. doi:10.1016/j.scs.2019.101827

Jensen, J. N. (2003). *A Problem Solving Approach to Aquatic Chemistry*. Hoboken, New Jersey, United States: John Wiley & Sons, 585.

Khan, A. U., and Rawat, B. P. (1990). Quaternary Geology and Geomorphology of a Part of Ganga basin in Parts of Bareilly, Badaun, Shahjahanpur and Pilibhit District, Uttar Pradesh. G.S.I. *Rec. Geol. Surv. India* 123 (8), 73–75.

Khan, M. A., and Wen, J. (2021). Evaluation of Physicochemical and Heavy Metals Characteristics in Surface Water under Anthropogenic Activities Using Multivariate Statistical Methods, Garra River, Ganges Basin, India. *Environ. Eng. Res.* 26 (6), 200280. doi:10.4491/eer.2020.280

Khan, M. Y. A. (2018). in *Handbook of Environmental Materials Management*. Editor C. M. Hussain (Berlin, Germany: Springer).*Spatial Variation in the Grain Size Characteristics of Sediments in Ramganga River, Ganga Basin, India*

Khan, M. Y. A., Hasan, F., Panwar, S., and Chakrapani, G. J. (2016). Neural Network Model for Discharge and Water-Level Prediction for Ramganga River Catchment of Ganga Basin, India. *Hydrological Sci. J.* 61 (11), 2084–2095. doi:10.1080/02626667.2015.1083650

Khan, M. Y. A., Hasan, F., and Tian, F. (2019). Estimation of Suspended Sediment Load Using Three Neural Network Algorithms in Ramganga River Catchment of Ganga Basin, India. *Sustain. Water Resour. Manag.* 5 (3), 1115–1131. doi:10.1007/s40899-018-0288-7

Krishnaswami, S., and Singh, S. K. (1998). Silicate and Carbonate Weathering in the Drainage Basins of the Ganga-Ghaghara-Indus Head Waters: Contributions to Major Ion and Sr Isotope Geochemistry. *Proc. Indian Acad. Sci. (Earth Planet. Sci.* 107 (4), 283–291. doi:10.1007/bf02841595

Kumar, A., Taxak, A. K., Mishra, S., and Pandey, R. (2021). Long Term Trend Analysis And Suitability Of Water Quality Of River Ganga At Himalayan Hills Of Uttarakhand, India. *Environ. Tech. Innov.* 22, 101405.

Lang, Y.-C., Liu, C.-Q., Zhao, Z.-Q., Li, S.-L., and Han, G.-L. (2006). Geochemistry of Surface and Ground Water in Guiyang, China: Water/rock Interaction and Pollution in a Karst Hydrological System. *Appl. Geochem.* 21 (6), 887–903. doi:10.1016/j.apgeochem.2006.03.005

Li, Z., Xiao, J., Evaristo, J., and Li, Z. (2019). Spatiotemporal Variations in the Hydrochemical Characteristics and Controlling Factors of Streamflow and Groundwater in the Wei River of China. *Environ. Pollut.* 254, 113006. doi:10.1016/j.envpol.2019.113006

Liu, J., and Han, G. (2020). Distributions and Source Identification of the Major Ions in Zhujiang River, Southwest China: Examining the Relationships between

Human Perturbations, Chemical Weathering, Water Quality and Health Risk. *Expo. Health* 12 (4), 849–862. doi:10.1007/s12403-020-00343-y

Meybeck, M. (1979). Concentrations des eauxfluvialesen elements 'le majeurs et apportsen solution aux oceans. Rev. *Geol. Dyn. Geogr. Phys.* 21, 215–246.

Meybeck, M. (2003). Global Occurrence of Major Elements in Rivers. *Treatise Geochem.* 5, 605. doi:10.1016/b0-08-043751-6/05164-1

Meyer, K. J., Carey, A. E., and You, C.-F. (2017). Typhoon Impacts on Chemical Weathering Source Provenance of a High Standing Island Watershed, Taiwan. *Geochimica et Cosmochimica Acta* 215, 404–420. doi:10.1016/j.gca.2017.07.015

Mishra, S., Kumar, A., and Shukla, P. (2021). Estimation Of Heavy Metal Contamination In The Hindon River, India: An Environmetric Approach. *Appl. Water Sci.* 11 (1), 1–9.

Pacheco, F., and van der Weijden, C. H. (1996). Contributions of Water-Rock Interactions to the Composition of Groundwater in Areas with a Sizeable Anthropogenic Input: A Case Study of the Waters of the Fundão Area, Central Portugal. *Water Resour. Res.* 32 (12), 3553–3570. doi:10.1029/96wr01683

Pande, P. C., Vibhuti, V., Awasthi, P., Bargali, K., and Bargali, S. S. (2016). Agro-biodiversity of Kumaun Himalaya, India: a Review. *Curr. Agri Res. Jour* 4 (1), 16–34. doi:10.12944/carj.4.1.02

Panwar, S., Khan, M. Y. A., and Chakrapani, G. J. (2016). Grain Size Characteristics And Provenance Determination Of Sediment And Dissolved Load Of Alaknanda River, Garhwal Himalaya, India. *Environ. Earth Sci.* 75 (2), 1–15. doi:10.1007/s12665-015-4785-9

Panwar, S., Yang, S., Srivastava, P., Khan, M. Y. A., Sangode, S. J., and Chakrapani, G. J. (2020). Environmental Magnetic Characterization of the Alaknanda and Ramganga River Sediments, Ganga basin, India. *Catena* 190, 104529. doi:10.1016/j.catena.2020.104529

Rai, S. K., Singh, S. K., and Krishnaswami, S. (2010). Chemical Weathering in the plain and Peninsular Sub-basins of the Ganga: Impact on Major Ion Chemistry and Elemental Fluxes. *Geochimica et Cosmochimica Acta* 74 (8), 2340–2355. doi:10.1016/j.gca.2010.01.008

Shrivastava, V. K. (1999). *Commercial Activities and Development in the Ganga Basin*. New Delhi: Concept publishing company, 58.

Singh, S. K., Kumar, A., and France-Lanord, C. (2006). Sr and 87Sr/86Sr in Waters and Sediments of the Brahmaputra River System: Silicate Weathering, CO2 Consumption and Sr Flux. *Chem. Geology.* 234, 308–320. doi:10.1016/j.chemgeo.2006.05.009

Singh, S. K., Rai, S. K., and Krishnaswami, S. (2008). Sr And Nd Isotopes In River Sediments From The Ganga Basin: Sediment Provenance And Hotspots Of Physical Erosion. *J. Geophy. Res.* 113, F03006. doi:10.1029/2007JF000909

Sinha, D. K., Saxena, S., and Saxena, R. (2006). Seasonal Variation in the Aquatic Environment of Ramganga River at Moradabad: A Quantitative Study. *Indian J. Environ. Prot.* 26 (6), 488.

Szramek, K., McIntosh, J. C., Williams, E. L., Kanduc, T., Ogrinc, N., and Walter, L. M. (2007). Relative Weathering Intensity of Calcite versus Dolomite in Carbonate-Bearing Temperate Zone Watersheds: Carbonate Geochemistry and Fluxes from Catchments within the St. Lawrence and Danube River Basins. *Geochem. Geophys. Geosyst.* 8 (4), Q04002. doi:10.1029/2006GC001337

Tripathi, J. K., Ghazanfari, P., Rajamani, V., and Tandon, S. K. (2007). Geochemistry of Sediments of the Ganges Alluvial plains: Evidence of Large-Scale Sediment Recycling. *Quat. Int.* 159 (1), 119–130. doi:10.1016/j.quaint.2006.08.016

Tsering, T., Abdel Wahed, M. S. M., Iftekhar, S., and Sillanpää, M. (2019). Major Ion Chemistry of the Teesta River in Sikkim Himalaya, India: Chemical Weathering and Assessment of Water Quality. *J. Hydrol. Reg. Stud.* 24, 100612. doi:10.1016/j.ejrh.2019.100612

Conflict of Interest: The authors declare that the research was conducted in the absence of any commercial or financial relationships that could be construed as a potential conflict of interest.

Publisher's Note: All claims expressed in this article are solely those of the authors and do not necessarily represent those of their affiliated organizations, or those of the publisher, the editors, and the reviewers. Any product that may be evaluated in this article, or claim that may be made by its manufacturer, is not guaranteed or endorsed by the publisher.